

R2D2: Relational Text Decoding with Transformers

Aryan Arbabi
University of Toronto
Vector Institute

arbabi@cs.toronto.edu {mingqiuwang, dunan, shafey, izhak}
@google.com

Mingqiu Wang and Laurent El Shafey
and Nan Du and Izhak Shafran
Google Research

Abstract

We propose a novel framework for modeling the interaction between graphical structures and the natural language text associated with their nodes and edges. Existing approaches typically fall into two categories. One group ignores the relational structure by converting them into linear sequences and then utilize the highly successful Seq2Seq models. The other side ignores the sequential nature of the text by representing them as fixed-dimensional vectors and apply graph neural networks. Both simplifications lead to information loss.

Our proposed method utilizes both the graphical structure as well as the sequential nature of the texts. The input to our model is a set of text segments associated with the nodes and edges of the graph, which are then processed with a transformer encoder-decoder model, equipped with a self-attention mechanism that is aware of the graphical relations between the nodes containing the segments. This also allows us to use BERT-like models that are already trained on large amounts of text.

While the proposed model has wide applications, we demonstrate its capabilities on data-to-text generation tasks. Our approach compares favorably against state-of-the-art methods in four tasks without tailoring the model architecture. We also provide an early demonstration in a novel practical application – generating clinical notes from the medical entities mentioned during clinical visits.

1 Introduction

Many applications in natural language processing require modeling snippets of texts whose relationships are best represented by graphical structures. In other words, they can be viewed as graphical networks whose nodes and edges are labeled with textual descriptions, such as knowledge graphs (Ji et al., 2020) or the dialogue states in goal oriented dialog systems (Chen et al., 2017; Gao et al., 2018).

One exemplar task is the data-to-text (D2T) generation, which aims at generating textual descriptions of input structured data. This task has attracted increasing research interest, accordingly several public datasets and challenges with different levels of complexity have been created. *WikiBio* (Liu et al., 2018a) and *E2E* (Dušek et al., 2020) have relatively simple input structure consisting of key-value pairs, where the goal is to create a snippet that describes associated biographies and restaurants respectively. *AGENDA* (Koncel-Kedziorski et al., 2019) and *WebNLG* (Gardent et al., 2017), on the other hand, have more complex input graphs where the goal is to generate associated scientific abstracts, and natural language descriptions of given relations, respectively.

Current techniques for tasks such as D2T generally fall into two categories. On one side, the input graph is converted into a flat sequence, on which sequence-to-sequence (Seq2Seq) models (Sutskever et al., 2014) are employed. For example on the WebNLG dataset, where the graph relations are represented as (head, predicate, tail) tuples, one approach flattens the graph by concatenating the tuples, where the heads, predicates and tails are separated by special tokens (Harkous et al., 2020; Gardent et al., 2017; Ferreira et al., 2019). In a more elaborate approach, the input tree is traversed in a preferred order, and the branching structure is encoded using brackets (Moryossef et al., 2019). While flattening the graph has been shown to be effective for modeling simple structures, the resulting sequences are not unique. The order of the tuples are often arbitrary and nodes that belong to multiple tuples may be represented multiple times in the sequence. In short, these methods do not utilize the relational structure effectively.

An alternative direction (Koncel-Kedziorski et al., 2019) focuses on the graphical structure and exploits recent advances in graph neural network (GNN) architectures (Wu et al., 2020). The textual

descriptions are represented as fixed-dimensional vectors, for example by using the last state of a recurrent neural network (RNN). The node embeddings are initialized using these fixed vectors and the structure is modeled using a transformer-based GNN (Veličković et al., 2018). Since the texts are only utilized for initializing the node embeddings, the textual information is not fully retained and they do not generalize well. This weakness could be mitigated by resorting to copy mechanism where the decoder is allowed to copy portions of the input (See et al., 2017).

In this work we propose a novel approach that utilizes the graphical structure of the data, while having access to the full sequences of text associated with graph components. We utilize the transformer-based models (Vaswani et al., 2017), whose self-attention layers and multi-head attention mechanism have proven their versatility in modeling both the natural language (Devlin et al., 2018; Brown et al., 2020) and graphical structures (Veličković et al., 2018). After a preprocessing step that moves the original predicate texts (edge annotations) to newly added nodes, the new graph, whose predicates are now from a small closed set, is processed by our model. Our model, which can be viewed as an extension to the original transformer, is capable of processing multiple text segments (each corresponding to one node), while also utilizing the relations between the segments using a segment-wise attention mechanism. In another perspective, our model can be viewed as an attention-based graph neural network, where higher order relations between nodes (represented as text segments in the input) are utilized by stacking multiple attention layers in the transformer model.

Our model has several advantages to previous methods for data-to-text generation tasks. First, our method does not require linearizing the input structure and can, hence, better incorporate the relational information of the data, whose importance increases with the complexity of the input structure and the scarcity of the training data. Second, compared to previous GNN-based methods like Graph-Writer (Koncel-Kedziorski et al., 2019), we use a single transformer model for encoding both the relational information and the textual labels, eliminating the need for auxiliary encoders to encode textual labels to fixed-dimensional vectors (losing information), or relying on copy mechanism to generalize to unseen terms. Third, compared to

the more traditional pipeline methods (Shen et al., 2019; Moryossef et al., 2019; Dušek et al., 2020), our model is fully end-to-end and does not require additional steps such as content selection, delexicalization, etc. Fourth, our architecture choices allow us to initialize the proposed model with a BERT-like (Devlin et al., 2018) pretrained masked language model, such as XLNet (Yang et al., 2019) in our experiments, to take advantage of unsupervised training on large corpora and the resulting improvements in generalization.

2 Methods

2.1 Overview and task definition

A standard graph structure can be described as a collection of tuples of the form – (head, predicate, tail) – where the heads and the tails collectively form the nodes in the graph and predicates correspond to the labels of the edges. The scope of our work involves graphs whose nodes, and possibly edges, are annotated with text labels. Broadly, our goal is to infer the text associated with one or more target nodes, given the rest of the information in the graph. For example, in D2T tasks the goal is to infer the text that describes a given input graph. In this case, we regard the target text as the label for an extra dummy node. In general, the target nodes could be any subset of nodes in the graph.

The input graphs for different tasks may vary widely in format and characteristics. Often, we need to transform them into a structure that is compatible with our framework (or is more efficient). If the predicates are text sequences from an open set (or a large closed set), then we convert the input graph into its equivalent Levi graph (Levi, 1942), similar to the preprocessing step also used by Beck et al. (2018). This is done by adding a new node for each tuple, having the predicate as the text associated to the new node, effectively breaking the original tuples such as (head, predicate, tail) into two new tuples – (head, "head-to-predicate", predicate) and (predicate, "predicate-to-tail", tail). We refer to Figure 1 for an illustration of such a transformation. After our transformation, every node, including the newly added ones, corresponds to a text snippet, which we call a *text segment*, and the edges between them (the new predicates) form a closed categorical set. For the rest of the paper, unless specified, we are always referring to the transformed version of the graph.

More formally, given a set of N_X text segments

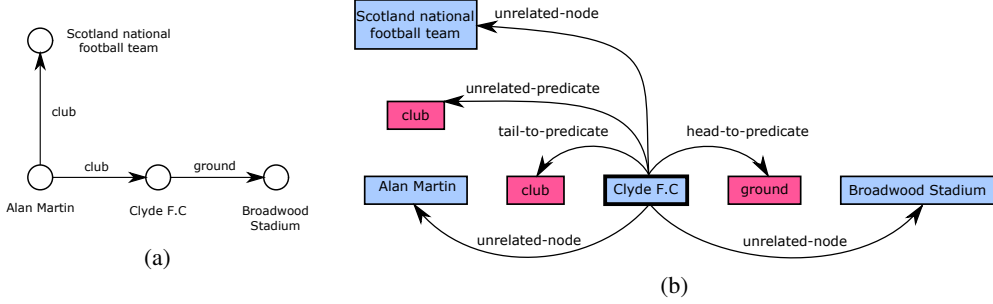


Figure 1: The plot on the left (a) depicts a graph example in its original format, where the predicates can have text labels from an open set. The plot on the right (b) shows the transformed version, where we have only depicted the relations originating from one specific node: “Clyde F.C”. The new graph is a network of text segments, each segment either being of the type “node” or “predicate”, colored in blue and pink respectively.

$X = \{s_i : 1 \leq i \leq N_X\}$ as source, our goal is to predict the set of N_Y target text segments $Y = \{s_i : N_X < i \leq N_X + N_Y\}$. Each text segment is itself a sequence of tokens, where the t -th token for the i -th segment is notated as $s_{i,t}$.

Each segment also has a categorical segment type (out of K possible types), notated as $B = (b_1, \dots, b_{N_X+N_Y})$. For example, one can allocate two segment types “node” and “predicate”, differentiating segments that correspond to the original nodes from the ones added to replace the original predicates in the Levi graph transformation.

We are also given a closed set of predicates Q (either original predicates or new ones the after graph transformation), and a set of tuples:

$$T = \{(s_{\text{head}_i}, q_i, s_{\text{tail}_i}) : 1 \leq i \leq N_T; s_{\text{head}_i}, s_{\text{tail}_i} \in X \cup Y; q_i \in Q\}.$$

We define an additional set of relations L , that supplements Q to cover segment pairs that do not form any tuple. L can have members such as “same-segment” for relations between each segment and itself, or “unrelated” for two unrelated ones. The underlying relational structure between the segments can then be represented by an adjacency matrix $G \in (Q \cup L)^{(N_X+N_Y) \times (N_X+N_Y)}$, where:

$$G_{i,j} = \begin{cases} q, & \text{if } \exists q : (s_i, q, s_j) \in T \\ l_{i,j} \in L, & \text{otherwise.} \end{cases}$$

We should note that we have assumed each pair of segments can have at most one predicate in T , and the relations can be directional (i.e. it is possible that $G_{i,j} \neq G_{j,i}$).

Our goal is to estimate $P(Y | X, B, G)$, where we call the set of variables (X, Y, G, B) the data schema. Characteristics of our model and its architecture are provided Section 2.2. We should also

note that the choice of the supplementary relations L and the segment types (b_i s) are design decisions and can vary across tasks. We have provided details of such design choices for our experiments Appendix A.

While D2T tasks only require inferring one target segment, our approach is more general and can infer multiple target segments, which may have other applications such as completing the missing nodes in knowledge graphs. Although it should be noted that due to the autoregressive nature of the generation process, each target segment can observe its relations only to the previously generated segments (in addition to the source segments).

2.2 Model architecture

We model $P(Y | X, B, G)$ with a conditional autoregressive model, parameterized by a transformer based on the XLNet-large architecture (Yang et al., 2019). XLNet is a masked language model used for unsupervised pretraining, a variant in the family of BERT (Devlin et al., 2018) style models, with the primary distinction of having an autoregressive decoding mechanism (opposed to the parallel decoding in other BERT variants). To enable this, for each target token two parallel streams are passed, one is given a special query symbol as input and predicts the real token, while the other is given the real token and processes it as context for decoding future tokens. See Figure 2 for an overview.

The autoregressive nature of XLNet is desirable for our framework, as we are also interested in using our model to decode target segments autoregressively. On the other hand, compared to entirely autoregressive models such as GPT-2 (Radford et al., 2019), XLNet has the advantage of applying a bidirectional attention over the source segments.

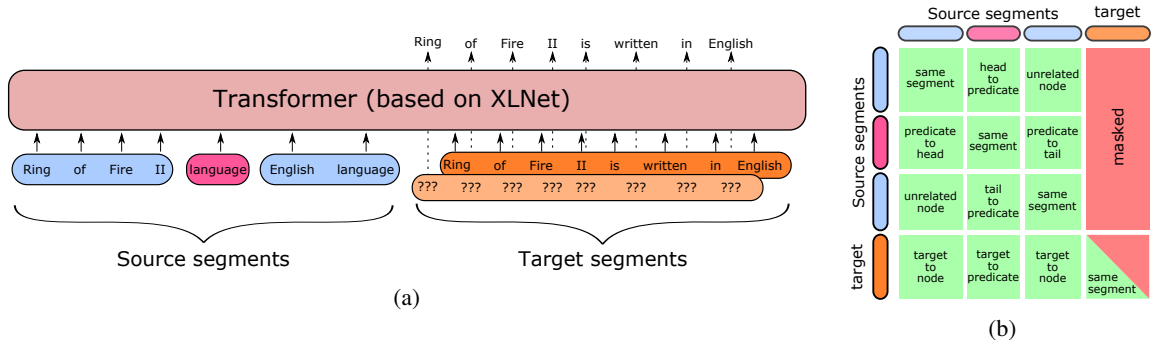


Figure 2: (a) R2D2 Architecture based on the XLNet model. The input is the concatenation of all text segments, where the blue, pink and orange segments correspond to node, predicate and target segment types. The model predicts the target tokens autoregressively, using a two-stream self-attention mechanism, with a *query-stream* colored in lighter orange passing a query "???" token, while the darker colored *content-stream*, passes the target tokens (ground truth tokens during the training or the previously decoded tokens during the inference) as context for generating future tokens. (b) The self-attention between segment pairs. Each row corresponds to one segment as query, attending to other segments (columns) as keys. The colors show if the key is visible (green) or hidden (red) to the query, while the cell labels indicate the relation type, which influences the segment-wise attention scores.

Another important advantage of XLNet is the use of relative segment embedding, in contrast to the absolute segment embedding employed in other BERT variants. To avoid confusion, we should remind that segment embedding and positional embedding are two different concepts; the former helps attending to the entirety of a segment (node), whereas the latter attends at the token level. The relative segment embedding is a more suitable approach for modeling texts in complex graphical structures, as explained further in Section 2.3.

The input to our model consists of the concatenation of all source and target segments. Any concatenation order would be fine, as the model is invariant to the order of the segments. However, in case of having multiple target segments, an order should be given for the autoregressive generation process. The model does not ignore the boundary of the segments nor the inter-segment relations, as these aspects are modeled through the relative attention mechanisms implemented in XLNet, which is further explained in Section 2.3.

While we use XLNet’s embedding table to embed the sequence tokens, we also learn another embedding table for the segment types. The segment type (b_i) and the token ($s_{i,t}$) embeddings are then summed to provide the final representation of each input token fed to the transformer.

2.3 Multi Segment Self-Attention

Pretrained transformer models such as BERT usually allow having multi-segment inputs (usually limited to two segments), to help with tasks such as

question answering where the context passage and the question can be marked as separate segments.

BERT and most of its other variations employ a global segment embedding for each of the two segment types (e.g. context and question) and add it to the input embedding to let the model know which tokens belong to which segment. In contrast, XLNet uses a relative segment embedding approach, where the attention score between two positions is affected by whether they both belong to the same segment or not, enabling each transformer cell to decide which segment to attend to.

In this work, we extended the relative segment embedding to more than two segments, where the inter-segment attention depends on the type of relation between pairs of segments. The attention score between any two positions has three components: 1) content-wise, 2) position-wise and 3) segment-wise. The scores of all three are summed to compute the final attention score. Figure 3 shows an example for the three attention components.

Consider we are calculating the attention score for the query token i at position t_i of the segment s_i and the key token j at position t_j of segment s_j . Further assume at the current layer of the transformer, the query and key vector for i and j are h_i^q and h_j^k respectively. The content-wise attention score is then calculated as:

$$a_{i,j}^{\text{content}} = (h_i^q + \phi_c)^T h_j^k. \quad (1)$$

where ϕ_c is a learnable bias parameter.

To calculate the segment-wise attention, we learn a table of relation-type embedding $H \in$

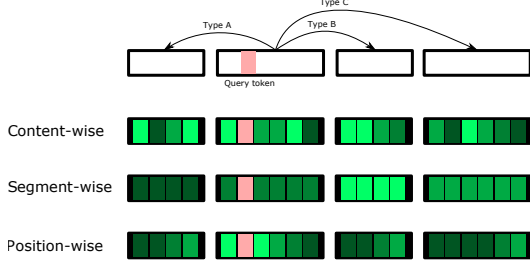


Figure 3: Multi-segment attention. The first row shows the structure of the text segments. The next three rows illustrate attention scores for each of the content-wise, segment-wise and position-wise components respectively. The shade of the green reflects the magnitude of the score. Note that every token of each segment shares the same segment-wise score, while for the position-wise attention the three external segments share the same pattern of attention from right to left.

$\mathbb{R}^{(|Q|+|L|)\times d}$, where each row corresponds to one relation category and d is the embedding dimension. Assuming σ_i and σ_j are the segment indices for s_i and s_j , the segment-wise attention score between i and j is derived as:

$$a_{i,j}^{\text{segment}} = (h_i^q + \phi_b)^T H_{G_{\sigma_i, \sigma_j}}. \quad (2)$$

The positional attention score is computed using a table of relative positional embedding R , where $R_{\tau(i,j)}$ is the embedding for the relative position between t_i and t_j and $\tau(i,j)$ is the relative position of t_i and t_j . If the two positions are located in the same segment, then deriving $\tau(i,j)$ would be straightforward as the relative position is simply the positional difference. However if the two belong to different segments, then given the absence of an underlying global positioning, the relative position between the two requires a new definition. We calculate the relative position between the tokens i and j as if their respective segments are concatenated as $[s_j, s_i]$. More formally:

$$\tau(i,j) = \begin{cases} t_i - t_j, & \text{if } \sigma_i = \sigma_j \\ t_i - t_j + |s_j|, & \text{otherwise.} \end{cases} \quad (3)$$

The positional attention score can be then derived as:

$$a_{i,j}^{\text{pos}} = (h_i^q + \phi_p)^T R_{\tau(i,j)}. \quad (4)$$

We should note that the reason we are using relative positional embedding in the first place is simply for compatibility with the pretrained XL-Net model, otherwise our model could also utilize

absolute positional embedding, where the leftmost token of each segment is viewed as having the absolute position 1, and tokens from different segments sharing the same absolute position are differentiated based on the content-wise and segment-wise attentions.

The final attention score is simply the sum of all three components:

$$a_{i,j} = a_{i,j}^{\text{content}} + a_{i,j}^{\text{segment}} + a_{i,j}^{\text{pos}}. \quad (5)$$

3 Experiments

3.1 Tasks

We evaluated our model on a range of tasks related to data-to-text generation, which includes WikiBio (Lebret et al., 2016), with 728k infobox-biography pairs from English Wikipedia, E2E challenge (Dušek et al., 2020) with 50k examples in the restaurant reservation domain, AGENDA (Koncel-Kedziorski et al., 2019), with 40k scientific abstracts, each supplemented with a title and a matching knowledge graph, and WebNLG (Gardent et al., 2017), containing 25k graph-text pairs, with graphs consisting of tuples from DBpedia and text being a verbalization of the graph. On all datasets we repeated our experiments (including the training process) three times and summarized our results by reporting the mean and variance of each metric.

The AGENDA and WebNLG tasks involve more complex graphs as their source, presented as general sets of tuples of the form (head, predicate, tail). The two, however, differ on the set of their permitted predicates: AGENDA comes with a closed set of seven predicate types, while the WebNLG predicates are arbitrary texts, comprising an open set. For both tasks, we grant one text segment per node, whereas for the predicates, we simply use the original seven possible predicates in AGENDA as distinct categories, while for WebNLG, we perform the Levi graph transformation and allocate additional text segments for the predicates, connecting them to their associated head and tail segments as illustrated in Figure 1. See Appendix A for task-specific data/graph preparation details.

3.2 Baselines

We compared our method with the current state-of-the-art models on each task (chosen based on the BLEU-4 score) and performed ablation studies to understand the impact of different components of our model.

We did ablation studies with four variants of our model. In the "scratch" variant, the model architecture was kept the same as XLNet but the parameters were initialized with random values and learned from scratch. In the "flattened" variant, the input structure was converted into a sequence by separating the different components of the relations – heads, tails, predicates, keys, values – with special tokens. In the "SF" variant, we both trained from scratch and flattened the input. Finally, the regular R2D2 is our proposed variant, utilizing both the pretrained weights and the graphical structure.

Current state-of-the-art model on WikiBio is the Structure Aware model introduced by Liu et al. (2018b). Their method flattens the input into two parallel sequences of keys and values. They are then processed in a Seq2Seq framework, where the LSTM decoder is augmented with a dual attention mechanism. They compute and sum two attention scores for each of the two sequences. Current state-of-the-art model on E2E is the Pragmatically Informative model of Shen et al. (2019), which is a Seq2Seq model whose input is delexicalized. During inference, they combine multiple scores in a beam search. The state-of-the-art model on AGENDA, the GraphWriter (Koncel-Kedziorski et al., 2019), uses an RNN encoder to map each text label into a fixed-dimension vector, which are then fed to a GNN model to process the graph. A decoder uses the output of the GNN as context and generates the target sequence. The decoder can also access the input text via a copy mechanism. Current state-of-the-art for WebNLG is the recent DataTurner model proposed by Harkous et al. (2020). They fine-tune the pre-trained GPT-2 model (Radford et al., 2019), which is shared between the encoder and the decoder. The input to the model is a flattened version of the graph.

3.3 Results

The results of our experiments on WikiBio are reported in Table 1, which show that our model outperforms the state-of-the-art (Liu et al., 2018b) with a considerable margin on both BLEU-4 and ROUGE-4 scores. The results for the E2E experiments are reported in Table 2, which show that our model is comparable to the state-of-the-art (Shen et al., 2019) model; we observe a small improvement in terms of NIST, METEOR, ROUGE-L and CIDEr, but with a slight reduction in BLEU-4 score. On WebNLG task, as reported in Table 3,

Method	BLEU-4	ROUGE-4
StructureAware*	44.89 ±0.33	41.65 ±0.25
R2D2	46.23 ±0.15	45.10 ±0.28
R2D2 (Flattened)	45.62 ±0.73	45.56 ±0.33
R2D2 (Scratch)	44.33 ±0.53	44.22 ±0.33
R2D2 (SF)	44.01 ±0.65	43.89 ±0.38
Reduced training set (R2D2) (number of samples / percent of training data)		
R2D2 (70k / 12%)	44.40 ±0.12	44.25 ±0.07
R2D2 (5k / 1%)	37.19 ±0.15	39.08 ±0.43
R2D2 (.5k / 0.1%)	33.00 ±0.82	34.10 ±0.42

Table 1: Results on the WikiBio task. State-of-the-art (Liu et al., 2018b) is notated by *.

our model performs comparably to the state-of-the-art model (Harkous et al., 2020), achieving a small improvement in BLEU-4 score and a slight reduction on the METEOR metric. Our results on the AGENDA task, reported in Table 4, show that our model outperforms the baseline (GraphWriter) (Koncel-Kedziorski et al., 2019) model by a considerable margin. Full results of our few-shot experiments, which includes all variants of R2D2, is available in Appendix B.

4 Discussion

The main benefits of our model come from three aspects: 1) encoding the graphical structure explicitly using the segment-wise attention mechanism; 2) concurrently modeling both the graphical structure and the text labels within a single transformer architecture, where the encoded text representations retain their full sequential information and length; 3) utilizing a pretrained language model like XLNet, trained on large amounts of data.

4.1 Pretraining and few shot learning

Our ablation studies show that without using the pretrained model, experiments on relatively small datasets such as AGENDA, E2E and WebNLG performed significantly worse, while this performance gap is much smaller for larger datasets such as WikiBio. Note, for experimental efficiency, we used the same large architecture for all tasks and smaller models for the smaller tasks may have avoided overfitting and improved performance.

The baseline model for the WebNLG task, the DataTurner model (Harkous et al., 2020), also uses a pretrained GPT-2 (Radford et al., 2019) model. GPT-2 is a fully autoregressive model, as such its

Method	BLEU-4	NIST	METEOR	ROUGE-L	CIDEr
PragInfo*	68.60	8.73	45.25	70.82	2.37
R2D2	67.70 \pm 0.64	8.68 \pm 0.10	45.85 \pm 0.18	70.44 \pm 0.32	2.38 \pm 0.04
R2D2 (Flattened)	65.73 \pm 0.97	8.48 \pm 0.13	45.29 \pm 0.24	70.21 \pm 0.73	2.32 \pm 0.05
R2D2 (Scratch)	52.25 \pm 2.45	7.31 \pm 0.16	37.40 \pm 1.05	60.13 \pm 1.76	1.34 \pm 0.08
R2D2 (SF)	52.25 \pm 3.56	7.24 \pm 0.21	36.66 \pm 2.10	58.97 \pm 1.91	1.31 \pm 0.07
Reduced training set (R2D2) (number of samples / percent of training data)					
R2D2 (4k / 10%)	67.01 \pm 0.65	8.65 \pm 0.06	45.26 \pm 0.30	69.48 \pm 0.60	2.29 \pm 0.06
R2D2 (1k / 2%)	63.93 \pm 1.13	8.46 \pm 0.11	43.90 \pm 1.18	66.95 \pm 0.76	2.15 \pm 0.07
R2D2 (.5k / 1%)	64.26 \pm 1.22	8.48 \pm 0.10	43.48 \pm 0.85	66.74 \pm 1.14	2.12 \pm 0.05

Table 2: Results on the E2E task. State-of-the-art (Shen et al., 2019) is notated by *.

Method	BLEU-4	METEOR
DataTurner*	52.9	41.9
R2D2	53.77 \pm 0.86	41.30 \pm 0.36
R2D2 (Flattened)	53.26 \pm 1.41	40.04 \pm 0.47
R2D2 (Scratch)	33.25 \pm 2.16	25.42 \pm 0.17
R2D2 (SF)	32.62 \pm 0.07	24.40 \pm 0.01
Reduced training set (R2D2) (number of samples / percent of training data)		
R2D2 (1.8k / 10%)	52.98 \pm 0.40	40.80 \pm 0.42
R2D2 (360 / 2%)	47.58 \pm 0.41	38.12 \pm 0.20
R2D2 (180 / 1%)	42.86 \pm 0.74	36.23 \pm 1.09

Table 3: Results on the WebNLG task. State-of-the-art (Harkous et al., 2020) is notated by *.

information flow, even on the source input, is unidirectional. In contrast our XLNet model has bidirectional information flow for the source input.

The results of our few-shot experiments show that the pretrained model can achieve relatively good results with reduced training data. More specifically, training on about 10% – 13% of the data from Wikibio (70k samples), E2E (4k samples), AGENDA (5k samples) and WebNLG (1.8k samples), led to a BLEU-4 score reduction of only 3.9%, 4%, 2.7%, and 0.3%, respectively, validating that low-resource data-to-text tasks can utilize transfer learning from large corpora.

4.2 Joint Encoding of Graph and Text

To understand the impact of our model explicitly encoding the graphical structure, we conducted ablation experiments by flattening the structured input into a linear sequence. This can be viewed as a regular Seq2Seq task. The loss of structural information resulted in .2%, 2.9%, 6.5%, 0.9% BLEU-4 score decrease on WikiBio, E2E, AGENDA, and WebNLG tasks respectively. As expected,

Method	BLEU-4	METEOR
GraphWriter*	14.3 \pm 1.01	18.8 \pm 0.28
R2D2	17.30 \pm 0.20	21.82 \pm 0.15
R2D2 (Flattened)	16.17 \pm 0.72	20.36 \pm 0.38
R2D2 (Scratch)	10.60 \pm 0.22	15.71 \pm 0.09
R2D2 (SF)	9.87 \pm 0.75	14.63 \pm 0.18
Reduced training set (R2D2) (number of samples / percent of training data)		
R2D2 (5k / 13%)	16.83 \pm 0.18	21.71 \pm 0.24
R2D2 (1k / 2.6%)	14.60 \pm 0.59	19.03 \pm 0.80
R2D2 (.5k / 1%)	13.00 \pm 0.38	17.59 \pm 0.19
R2D2 (.1k / 0.26%)	10.61 \pm 1.77	15.56 \pm 1.20

Table 4: Results on the AGENDA task. State-of-the-art (Koncel-Kedziorski et al., 2019) is notated by *.

AGENDA and WebNLG, which have more complex graph structures, showed a larger drop in performance when flattened, compared to WikiBio. More importantly, our ablation study shows that utilizing the graph structure can boost the performance independent of whether pretrained weights were used and the two have a complementary effect on the performance gain.

One surprising observation was that the graphical structure benefited the relatively simple E2E task too, where perhaps the structural information helped offset the data scarcity (compared to WikiBio). We further investigated this phenomenon by repeating the few shot experiments on the flattened version of the model. The performance gain from utilization of the graphical structure was indeed more significant in several few shot experiments, such as WebNLG where reducing the training data to 1800 samples led to 1.4% and 5.7% drops in BLEU score for the main variant and the flattened version respectively.

4.3 End-to-end Learning

State-of-the-art models for certain tasks have multiple steps such as delexicalization and second pass rescoring, as mentioned earlier (Shen et al., 2019; Moryossef et al., 2019; Dušek et al., 2020). Our model on the other hand is purely end-to-end without the hassles of delexicalization, copy mechanism, or other interventions. Consequently, all model components including those devoted to textual description and structural information can be trained simultaneously, affording an opportunity to achieve better overall performance.

4.4 Computational complexity

The computational cost of R2D2 would be similar to that of regular transformers, requiring $O(n^2)$ dot product computations per layer, where n is the total length of all text segments concatenated. Consequently, the framework would allow graphs that have less than n_{\max}/n_{seg} number of nodes, where n_{\max} is the maximum permitted sequence length for the transformer and n_{seg} is the average segment length. Accordingly, R2D2 is more suitable for tasks involving smaller graphs or local sub graphs.

5 Applications in clinical note generation

We applied our model to an early stage demonstration of a novel clinical application: generating clinical notes from extracted entities. This is motivated by the need to improve the accuracy and efficiency of clinical documentation (e.g., (Liu, 2018)), which takes an inordinate amount of time from clinicians after patient visits. With current capabilities of speech recognition and entity extraction, we could potentially extract the entities into a relevant data structure and then synthesize the clinical notes.

For this proof-of-concept demonstration, we used ICU discharge notes from the MIMIC-III dataset (Johnson et al., 2016). Each section was chunked into text snippets of at most 250 tokens. We then used an in-house entity extractor (Brown, 2013) to extract medical key-value pairs, such as symptom, medication, condition, etc. (see Figure 4). We used these key-value pairs as the input graph and the text snippet as the target text.

Automatic evaluation results on our validation set (5,765 samples) show scores of BLEU-4 18.43, NIST 1.7486, METEOR 0.1957, ROUGE-L, 0.3340, and CIDEr 0.0812. Figure 4 shows the snippet of an inferred clinical note. The model is able to capture information well from the input

Diagnostic Test	Symptom	Disease
EKG	Ischemia	Adverse Drug Reactions
Cardiac Catheterization	Syncope	Allergies
EKG	Palpitations	Coronary Artery Dissection
	Lightheadedness	Hyperlipidemia
Drug/Treatment		
Integrilin	ST Depression	Stress
Heparin	Orthopnea	Anginal
Angioplasty	Shortness Of Breath	CAD
Balloon Angioplasty	Medical Specialty	Atrial Fibrillation
	Surgical	

INPUT

Service: MEDICINE	OUTPUT
Allergies: No Known Allergies / Adverse Drug Reactions	
Attending: [**First Name3 (LF) 7055**]	
Chief Complaint: Coronary artery dissection	
Major Surgical or Invasive Procedure: Balloon angioplasty	
History of Present Illness: This is a 76 year old male with history of hypertension, hyperlipidemia, anginal symptoms, shortness of breath, and palpitations who underwent an EKG and ECG which revealed atrial fibrillation and was referred for balloon angioplasty.	

Figure 4: Clinical note generation with MIMIC-III data.

table. However when there is information in the target sequence for which the relevant entity/attributes are missing in the input, the model learns to hallucinate. Similarly, when attributes are missing from the input table, such as symptom negation, severity, etc., the model is confused whether to generate "patient denied symptoms" or "patient reported symptoms". Techniques such as forced copy mechanism might be necessary to safeguard against generating text that is not confidently supported by the input.

6 Conclusion

In this paper, we proposed a novel architecture for modeling the interaction between graphical structure where nodes (and possibly edges) contain descriptive text, and demonstrated performance gains over state-of-the-art models on the task of generating text from structured data. The framework allows us to exploit pretrained XLNet encoder and achieve relatively good performance even with small amounts of training data. Our ablation analysis showed that although using the pretrained model has a significant impact on the performance gain, utilizing the graphical information with the multi-level attention mechanism has a complementary effect and boosts the performance independent of whether pretrained weights were used. Our attempt to utilize this model in generating clinical notes hopefully inspires more work in this direction to solve a practical application of considerable importance.

References

- Daniel Beck, Gholamreza Haffari, and Trevor Cohn. 2018. Graph-to-sequence learning using gated graph neural networks. In *Proceedings of the 56th Annual Meeting of the Association for Computational Linguistics (Volume 1: Long Papers)*, pages 273–283.
- Aaron Brown. 2013. Semantics and structured knowledge in practice at Google. In *IEEE International Conference on Semantic Computing (ICSC)*.
- Tom B Brown, Benjamin Mann, Nick Ryder, Melanie Subbiah, Jared Kaplan, Prafulla Dhariwal, Arvind Neelakantan, Pranav Shyam, Girish Sastry, Amanda Askell, et al. 2020. Language models are few-shot learners. *arXiv preprint arXiv:2005.14165*.
- Hongshen Chen, Xiaorui Liu, Dawei Yin, and Jiliang Tang. 2017. A survey on dialogue systems: Recent advances and new frontiers. *ACM SIGKDD Explorations Newsletter*, 19(2):25–35.
- Jacob Devlin, Ming-Wei Chang, Kenton Lee, and Kristina Toutanova. 2018. BERT: Pre-training of deep bidirectional transformers for language understanding. In *Annual Conference of the North American Chapter of the Association for Computational Linguistics (NAACL)*.
- Ondřej Dušek, Jekaterina Novikova, and Verena Rieser. 2020. Evaluating the State-of-the-Art of End-to-End Natural Language Generation: The E2E NLG Challenge. *Computer Speech & Language*, 59:123–156.
- Thiago Castro Ferreira, Chris van der Lee, Emiel van Miltenburg, and Emiel Kraemer. 2019. Neural data-to-text generation: A comparison between pipeline and end-to-end architectures. In *Conference on Empirical Methods in Natural Language Processing and International Joint Conference on Natural Language Processing (EMNLP-IJCNLP)*.
- Jianfeng Gao, Michel Galley, and Lihong Li. 2018. Neural approaches to conversational ai. In *International ACM SIGIR Conference on Research & Development in Information Retrieval*, pages 1371–1374.
- Claire Gardent, Anastasia Shimorina, Shashi Narayan, and Laura Perez-Beltrachini. 2017. The WebNLG challenge: Generating text from RDF data. In *International Conference on Natural Language Generation (INLG)*, pages 124–133.
- Hamza Harkous, Isabel Groves, and Amir Saffari. 2020. Have your text and use it too! end-to-end neural data-to-text generation with semantic fidelity. *arXiv preprint arXiv:2004.06577*.
- Shaoxiong Ji, Shirui Pan, Erik Cambria, Pekka Marttinen, and Philip S Yu. 2020. A survey on knowledge graphs: Representation, acquisition and applications. *arXiv preprint arXiv:2002.00388*.
- Alistair EW Johnson, Tom J Pollard, Lu Shen, H Lehman Li-wei, Mengling Feng, Mohammad Ghassemi, Benjamin Moody, Peter Szolovits, Leo Anthony Celi, and Roger G Mark. 2016. MIMIC-III, a freely accessible critical care database. *Scientific Data*, 3:160035.
- Rik Koncel-Kedziorski, Dhanush Bekal, Yi Luan, Mirella Lapata, and Hannaneh Hajishirzi. 2019. Text generation from knowledge graphs with graph transformers. In *Conference of the North American Chapter of the Association for Computational Linguistics (NAACL)*, pages 2284–2293.
- Rémi Lebret, David Grangier, and Michael Auli. 2016. Neural text generation from structured data with application to the biography domain. In *Conference on Empirical Methods in Natural Language Processing (EMNLP)*.
- Friedrich Wilhelm Levi. 1942. *Finite geometrical systems: six public lectures delivered in February, 1940, at the University of Calcutta*. University of Calcutta.
- Peter J Liu. 2018. Learning to write notes in electronic health records. *arXiv preprint arXiv:1808.02622*.
- Peter J Liu, Mohammad Saleh, Etienne Pot, Ben Goodrich, Ryan Sepassi, Lukasz Kaiser, and Noam Shazeer. 2018a. Generating Wikipedia by summarizing long sequences. *arXiv preprint arXiv:1801.10198*.
- Tianyu Liu, Kexiang Wang, Lei Sha, Baobao Chang, and Zhifang Sui. 2018b. Table-to-text generation by structure-aware seq2seq learning. In *Thirty-Second AAAI Conference on Artificial Intelligence*.
- Amit Moryossef, Yoav Goldberg, and Ido Dagan. 2019. Step-by-step: Separating planning from realization in neural data-to-text generation. In *Proceedings of the 2019 Conference of the North American Chapter of the Association for Computational Linguistics: Human Language Technologies, Volume 1 (Long and Short Papers)*, pages 2267–2277.
- Alec Radford, Jeff Wu, Rewon Child, David Luan, Dario Amodei, and Ilya Sutskever. 2019. Language models are unsupervised multitask learners.
- Abigail See, Peter J Liu, and Christopher D Manning. 2017. Get to the point: Summarization with pointer-generator networks. In *Annual Meeting of the Association for Computational Linguistics (ACL)*.
- Sheng Shen, Daniel Fried, Jacob Andreas, and Dan Klein. 2019. Pragmatically informative text generation. In *Conference of the North American Chapter of the Association for Computational Linguistics (NAACL)*.
- Ilya Sutskever, Oriol Vinyals, and Quoc V Le. 2014. Sequence to sequence learning with neural networks. In *Advances in neural information processing systems (NIPS)*, pages 3104–3112.

Ashish Vaswani, Noam Shazeer, Niki Parmar, Jakob Uszkoreit, Llion Jones, Aidan N Gomez, Łukasz Kaiser, and Illia Polosukhin. 2017. Attention is all you need. In *Advances in neural information processing systems*, pages 5998–6008.

Petar Veličković, Guillem Cucurull, Arantxa Casanova, Adriana Romero, Pietro Liò, and Yoshua Bengio. 2018. [Graph attention networks](#). In *International Conference on Learning Representations (ICLR)*.

Zonghan Wu, Shirui Pan, Fengwen Chen, Guodong Long, Chengqi Zhang, and S Yu Philip. 2020. A comprehensive survey on graph neural networks. *IEEE Transactions on Neural Networks and Learning Systems*.

Zhilin Yang, Zihang Dai, Yiming Yang, Jaime Carbonell, Ruslan Salakhutdinov, and Quoc V Le. 2019. XLNet: Generalized autoregressive pretraining for language understanding. In *Advances in Neural Information Processing Systems (NeurIPS)*.

A Dataset details and preparations

A.1 WikiBio

The WikiBio corpus (Lebret et al., 2016) comprises 728, 321 biography-infobox pairs from English Wikipedia (dumped in 2015). The task consists of generating the first sentence of a biography conditioned on the structured infobox. The average length of infoboxes and first sentences are 53.1 and 26.1 respectively. All tokens are lower-cased.

We associate a text segment for each key and value, and a separate segment for the target sentence. Five relation types were defined: 1) from a key/value to its paired value/key; 2) from a key/value/target to every other key except if the two belong to a key-value pair; 3) from a key/value/target to every other value except if the two belong to a key-value pair; 4) from a key/value to the target (these are masked); 5) from any segment to itself.

A.2 E2E

The E2E challenge is based on a crowd-sourced dataset of 50k samples in the restaurant domain. The task is to generate a description of a restaurant from structured input in the form of key-value pairs. We used a graph structure identical to the one explained for the WikiBio dataset.

A.3 AGENDA

AGENDA dataset (Koncel-Kedziorski et al., 2019) comprises 40, 720 scientific abstracts, each supplemented with the title and a matching knowledge graph. The knowledge graphs consist of entities and relations extracted from their corresponding abstract. The dataset is split into 38, 720 training, 1, 000 validation, and 1, 000 test datapoints. The average lengths of titles and abstracts are 9.5 and 141.2 tokens respectively. The goal of the task is to generate an abstract given the title and the associated knowledge graph as the source. The input graphs in this dataset can form more complex structures compared to WikiBio and E2E, which are limited to key-value pairs.

The knowledge graphs consists of a set of “*concepts*” and a set of predicates connecting them. There are seven predicate categories, namely: “Used-for”, “Feature-of”, “Conjunction”, “Part-of”, “Evaluate-for”, “Hyponym-for”, and “Compare”. Each concept is also assigned a *class*, out of five possible classes: “Task”, “Method”, “Metric”, “Material”, or “Other Scientific Term”. We also in-

corporate the given title in the knowledge graph as a concept and give its own class of *title-class*. Clearly, this new concept does not have any predicates connecting it to others.

We assign a text segment for each concept, class and target (the abstract), adding up to a total of three segment types. We also define a total of twelve types of relations, including the original seven predicate categories. The five supplementary relations are: 1) from a concept/class to its paired class/concept; 2) from a concept/class/target to every other concept unless the two are already linked; 3) from a concept/class/target to every other class except unless the two are already linked; 4) from a concept/class to the target (these are masked); 5) from any block to itself.

A.4 WebNLG

WebNLG dataset, curated from DB-Pedia, consists of sets of (head, predicate, tail) tuples forming a graphical structure and a descriptive target text verbalising them. The dataset consists of 25, 298 graph-text pairs, among which 9, 674 are distinct graphs (multiple targets for a graph produced by different crowdsourcing agents). In each graph there can be between one to seven tuples. The test data spans fifteen different domains, ten of which appear in the training data.

Both nodes (heads and tails) and the predicates are textual labels and the predicates are from an open set. As a result, we transform the graph to its Levi equivalent by allocating a new node per tuple with the predicate as its text label. This new graph has three types of text segments: nodes (original heads and tails), predicates (newly added nodes), and the target. There are seven types of relations in the new graph: 1) from a node segment to all predicate segments, for which the node was a head; 2) from a node segment to all predicate segments, for which the node was a tail; 3) from each node/predicate to all predicates, except if the two were linked by a tuple; 4) from each node to all other nodes (including the ones that are linked by a tuple) and from each predicate to all nodes except if the two are linked by a tuple; 5) from target to all node segments; 6) from target to all predicate segments; 7) from a segment to itself.

B Complete Experiment results

Full results of our experiments are provided in Table 5, Table 6, Table 7 and Table 8, for WikiBio,

E2E, WebNLG and AGENDA tasks respectively. For WebNLG and E2E we used the official evaluation scripts to compute the scores. We also used the popularly used ROUGE-1.5.5.pl to calculate the ROUGE-4 scores.

Method	BLEU-4	ROUGE-4
StructureAware*	44.89 \pm 0.33	41.65 \pm 0.25
R2D2	46.23 \pm 0.15	45.10 \pm 0.28
R2D2 (Flattened)	45.62 \pm 0.73	45.56 \pm 0.33
R2D2 (Scratch)	44.33 \pm 0.53	44.22 \pm 0.33
R2D2 (SF)	44.01 \pm 0.65	43.89 \pm 0.38
Reduced training set (R2D2) (number of samples / percent of training data)		
R2D2 (70k / 12%)	44.40 \pm 0.12	44.25 \pm 0.07
R2D2 (5k / 1%)	37.19 \pm 0.15	39.08 \pm 0.43
R2D2 (.5k / 0.1%)	33.00 \pm 0.82	34.10 \pm 0.42
Reduced training set (R2D2 Flattened) (number of samples / percent of training data)		
R2D2 (Flattened) (70k / 12%)	44.44 \pm 0.18	44.21 \pm 0.08
R2D2 (Flattened) (5k / 1%)	36.39 \pm 0.21	39.31 \pm 0.56
R2D2 (Flattened) (.5k / 0.1%)	30.53 \pm 1.09	31.60 \pm 0.98
Reduced training set (R2D2 - Scratch) (number of samples / percent of training data)		
R2D2 (Scratch) (70k / 12%)	43.16 \pm 0.34	42.67 \pm 0.44
R2D2 (Scratch) (5k / 1%)	34.48 \pm 0.51	33.40 \pm 0.79
R2D2 (Scratch) (.5k / 0.1%)	7.94 \pm 0.71	28.00 \pm 0.82
Reduced training set (R2D2 - Scratch and Flattened) (number of samples / percent of training data)		
R2D2 (SF) (70k / 12%)	42.96 \pm 0.25	41.87 \pm 0.31
R2D2 (SF) (5k / 1%)	33.18 \pm 0.34	29.81 \pm 0.50
R2D2 (SF) (.5k / 0.1%)	7.67 \pm 0.78	31.00 \pm 0.80

Table 5: Results on the WikiBio task. State-of-the-art (Liu et al., 2018b) is notated by *.

Method	BLEU-4	NIST	METEOR	ROUGE-L	CIDEr
PragInfo*	68.60	8.73	45.25	70.82	2.37
R2D2	67.70 \pm 0.64	8.68 \pm 0.10	45.85 \pm 0.18	70.44 \pm 0.32	2.38 \pm 0.04
R2D2 (Flattened)	65.73 \pm 0.97	8.48 \pm 0.13	45.29 \pm 0.24	70.21 \pm 0.73	2.32 \pm 0.05
R2D2 (Scratch)	52.25 \pm 2.45	7.31 \pm 0.16	37.40 \pm 1.05	60.13 \pm 1.76	1.34 \pm 0.08
R2D2 (SF)	52.25 \pm 3.56	7.24 \pm 0.21	36.66 \pm 2.10	58.97 \pm 1.91	1.31 \pm 0.07
Reduced training set (R2D2) (number of samples / percent of training data)					
R2D2 (4k / 10%)	67.01 \pm 0.65	8.65 \pm 0.06	45.26 \pm 0.30	69.48 \pm 0.60	2.29 \pm 0.06
R2D2 (1k / 2%)	63.93 \pm 1.13	8.46 \pm 0.11	43.90 \pm 1.18	66.95 \pm 0.76	2.15 \pm 0.07
R2D2 (.5k / 1%)	64.26 \pm 1.22	8.48 \pm 0.10	43.48 \pm 0.85	66.74 \pm 1.14	2.12 \pm 0.05
Reduced training set (R2D2 Flattened) (number of samples / percent of training data)					
R2D2 (Flattened) (4k / 10%)	65.15 \pm 0.74	8.64 \pm 0.05	44.38 \pm 0.91	68.71 \pm 1.18	2.22 \pm 0.08
R2D2 (Flattened) (1k / 2%)	63.76 \pm 0.49	8.50 \pm 0.08	43.35 \pm 0.51	66.92 \pm 0.98	1.63 \pm 0.84
R2D2 (Flattened) (.5k / 1%)	63.02 \pm 0.42	8.55 \pm 0.02	43.44 \pm 0.15	66.79 \pm 0.50	2.17 \pm 0.04
Reduced training set (R2D2 Scratch) (number of samples / percent of training data)					
R2D2 (Scratch) (4k / 10%)	52.86 \pm 1.05	7.14 \pm 0.12	37.69 \pm 1.41	60.00 \pm 0.48	1.15 \pm 0.02
R2D2 (Scratch) (1k / 2%)	52.72 \pm 0.21	7.21 \pm 0.15	34.78 \pm 0.93	57.33 \pm 0.74	1.26 \pm 0.03
R2D2 (Scratch) (.5k / 1%)	49.41 \pm 0.91	7.09 \pm 0.20	34.95 \pm 1.29	56.40 \pm 0.90	1.21 \pm 0.07
Reduced training set (R2D2 Scratch and Flattened) (number of samples / percent of training data)					
R2D2 (SF) (4k / 10%)	51.93 \pm 1.25	7.26 \pm 0.18	37.19 \pm 1.04	58.88 \pm 0.79	1.20 \pm 0.05
R2D2 (SF) (1k / 2%)	49.29 \pm 0.99	6.64 \pm 0.16	31.85 \pm 2.41	57.08 \pm 1.28	1.03 \pm 0.09
R2D2 (SF) (.5k / 1%)	45.29 \pm 0.37	6.72 \pm 0.27	33.42 \pm 1.98	54.34 \pm 2.03	1.07 \pm 0.06

Table 6: Results on the E2E task. State-of-the-art (Shen et al., 2019) is notated by *.

Method	BLEU-4	METEOR
DataTurner*	52.9	41.9
R2D2	53.77 ± 0.86	41.30 ± 0.36
R2D2 (Flattened)	53.26 ± 1.41	40.04 ± 0.47
R2D2 (Scratch)	33.25 ± 2.16	25.42 ± 0.17
R2D2 (SF)	32.62 ± 0.07	24.40 ± 0.01
Reduced training set (R2D2) (number of samples / percent of training data)		
R2D2 (1.8k / 10%)	52.98 ± 0.40	40.80 ± 0.42
R2D2 (360 / 2%)	47.58 ± 0.41	38.12 ± 0.20
R2D2 (180 / 1%)	42.86 ± 0.74	36.23 ± 1.09
Reduced training set (R2D2 Flattened) (number of samples / percent of training data)		
R2D2 (Flattened) (1.8k / 10%)	50.20 ± 0.34	39.00 ± 0.40
R2D2 (Flattened) (360 / 2%)	46.52 ± 0.62	36.97 ± 1.21
R2D2 (Flattened) (180 / 1%)	43.10 ± 0.64	35.19 ± 0.41
Reduced training set (R2D2 Scratch) (number of samples / percent of training data)		
R2D2 (Scratch) (1.8k / 10%)	30.09 ± 1.43	23.30 ± 0.35
R2D2 (Scratch) (360 / 2%)	22.59 ± 1.79	18.00 ± 1.29
R2D2 (Scratch) (180 / 1%)	19.93 ± 2.25	16.70 ± 1.98
Reduced training set (R2D2 Scratch and Flattened) (number of samples / percent of training data)		
R2D2 (SF) (1.8k / 10%)	29.20 ± 1.02	22.62 ± 0.29
R2D2 (SF) (360 / 2%)	19.18 ± 1.56	16.71 ± 0.95
R2D2 (SF) (180 / 1%)	18.64 ± 2.03	16.23 ± 1.75

Table 7: Results on the WebNLG task. State-of-the-art (Harkous et al., 2020) is notated by *.

Method	BLEU-4	METEOR
GraphWriter*	14.3 \pm 1.01	18.8 \pm 0.28
R2D2	17.30 \pm 0.20	21.82 \pm 0.15
R2D2 (Flattened)	16.17 \pm 0.72	20.36 \pm 0.38
R2D2 (Scratch)	10.60 \pm 0.22	15.71 \pm 0.09
R2D2 (SF)	9.87 \pm 0.75	14.63 \pm 0.18
Reduced training set (R2D2) (number of samples / percent of training data)		
R2D2 (5k / 13%)	16.83 \pm 0.18	21.71 \pm 0.24
R2D2 (1k / 2.6%)	14.60 \pm 0.59	19.03 \pm 0.80
R2D2 (.5k / 1%)	13.00 \pm 0.38	17.59 \pm 0.19
R2D2 (.1k / 0.26%)	10.61 \pm 1.77	15.56 \pm 1.20
Reduced training set (R2D2 Flattened) (number of samples / percent of training data)		
R2D2 (Flattened) (5k / 13%)	16.37 \pm 0.28	20.68 \pm 0.33
R2D2 (Flattened) (1k / 2.6%)	14.31 \pm 0.82	19.15 \pm 0.97
R2D2 (Flattened) (.5k / 1%)	12.58 \pm 0.14	16.84 \pm 0.02
R2D2 (Flattened) (.1k / 0.26%)	9.38 \pm 0.21	15.00 \pm 1.27
Reduced training set (R2D2 Scratch) (number of samples / percent of training data)		
R2D2 (Scratch) (5k / 13%)	9.45 \pm 0.31	14.69 \pm 0.22
R2D2 (Scratch) (1k / 2.6%)	3.21 \pm 1.21	8.56 \pm 0.10
R2D2 (Scratch) (.5k / 1%)	2.96 \pm 1.09	7.01 \pm 0.39
R2D2 (Scratch) (.1k / 0.26%)	2.70 \pm 0.79	6.77 \pm 0.76
Reduced training set (R2D2 Scratch and Flattened) (number of samples / percent of training data)		
R2D2 (SF) (5k / 13%)	7.98 \pm 0.12	14.01 \pm 0.55
R2D2 (SF) (1k / 2.6%)	3.18 \pm 0.69	8.81 \pm 0.72
R2D2 (SF) (.5k / 1%)	3.12 \pm 0.90	8.43 \pm 0.48
R2D2 (SF) (.1k / 0.26%)	2.31 \pm 1.79	5.70 \pm 1.25

Table 8: Results on the AGENDA task. State-of-the-art (Koncel-Kedziorski et al., 2019) is notated by *.